EARTHQUAKE OBSERVATION AND RESPONSE ANALYSIS OF SHIELD TUNNEL

by

Takeyasu Suzuki*, Choshiro Tamura**, Hiroshi Maeda***

ABSTRACT

The characteristic behaviors of a shield tunnel during earthquakes were recognized by the observation conducted by the authors. The response analysis, using quasi-three dimensional ground model, was executed and its results show good agreements with the observation.

INTRODUCTION

Recent progress in shield tunneling technology has enabled us to excavate and construct a tunnel even under unfavorable condition. A shield tunnel of large diameter (over 10 meters) has been developed. Its usage will be expanded, keeping pace with the improvement of traffic network. However, it has not yet experienced a large earthquake until now, because shield tunneling is comparatively a new method. Therefore, the establishment of its earthquake resistent design is an urgent necessity.

The authors have been executing earthquake observation[1,2] in order to clarify the mechanism of a seismicity of shield tunnels during earthquake since 1983. Detailed analyses of data obtained from the recent several earthquakes have brought about pieces of considerable information. In this paper, characteristic behaviors of the ground and tunnels during earthquakes are introduced. In addition, a response analysis using quasi-three dimensional ground model is carried out, and its results are compared with actual observation. They show good agreements and the importance of ground modeling technique was recognized.

OUTLINE OF OBSERVATION SITE

The observation site is located in the southern part of Yokohama City. Fig. 1 shows the topography of the observation site. As shown in Fig. 1, alluvial silty clay is sedimented inbetween two separate hills of deluvial mud stone, where a drawned valley is formed. The dotted line in this figure illustrates the boundary of mud stone at the level of tunnel bottom. The shield tunnel is constructed, crossing the valley at a low angle. The tunnel is used for electric power cable with the outer diameter of 5.1 meters. The tunnel is composed of reinforced concrete segments.

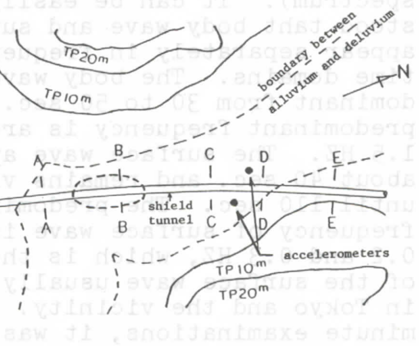

Fig. 1 Topographical Map of the Observation Site

Fig. 2 shows the cross section of the observation site. The

* Research Personnel, Institute of Construction Technology, Kumagai-Gumi, Co., Ltd.
** Professor, Institute of Industrial Science, University of Tokyo.
*** Deputy General Manager, Transmission and Transformation Facilities Construction Administration, The Tokyo Electric Power Co.,Inc.

ground movement is measured by accelerometers laid under the ground. Each accelerometer is arranged as shown in Fig. 1 and 2. The tunnel behavior is observed at tunnel sections from A through E, and strain meters are installed at each section both in the direction of tunnel axis and along tunnel inner circle. The shear wave velocity of alluvial clayey layer ranges from 40 to 260 m/sec., whereas that of the deluvial mud stone layer is about 750 m/sec.

OBSERVATION RESULTS

Since 1983, four major earthquakes out of the earthquakes recorded at the site have been selected for detailed analyses (see Table 1). In this chapter, the authors introduce the dynamic behaviors of the ground and tunnel due to the following two characteristic earthquakes. One is Naganoken-Seibu Earthquake, in which the surface wave is predominant. While, the body wave is predominant, in another one, Chiba-Ibaragi Kenkyo Earthquake.

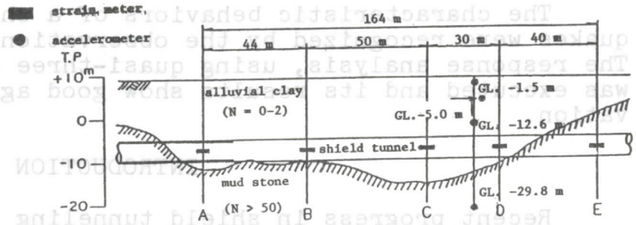

Fig. 2 Cross Section of the Observation Site

No.	Earthquake Name	Magnitude	Date	Epicentral Distance (km)
1.	Kanagawa-Yamanashi Kenkyo	6.0	8/ 8/83	60
2.	Torishima Kinkai	7.9	3/ 6/84	450
3.	Naganoken-Seibu	6.8	9/14/84	200
4.	Chiba-Ibaragi Kenkyo	6.2	10/ 4/85	61

Table 1 Major Earthquakes Recorded at the Site

Naganoken-Seibu Earthquake (No. 3 Earthquake)

Fig. 3 shows the acceleration record near the ground surface (GL. -1.5 m) and its evolutionary spectrum (multi-filter spectrum). It can be easily understood taht body wave and surface wave appear separately in frequency and time domains. The body wave is predominant from 30 to 50 sec. and the predominant frequency is around 1.5 HZ. The surface wave appears at about 40 sec. and remains visible until 110 sec. The predominant frequency of surface wave is between 0.2 and 0.3 HZ, which is the frequency of the surface wave usually observed in Tokyo and the vicinity. After minute examinations, it was estimated that this wave is Love Wave.

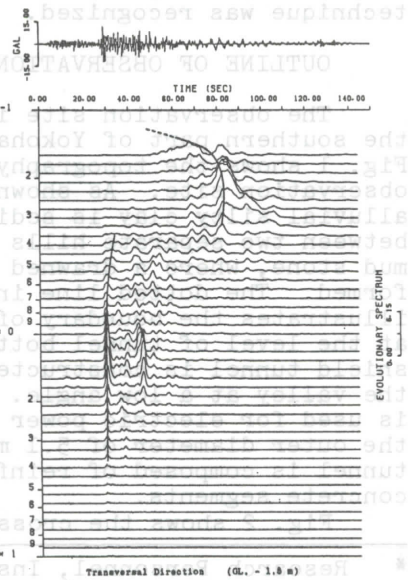

Fig. 3 Acceleration Record and its Evolutionary Spectrum

Fig. 4 shows tunnel axial strains due to this earthwuake. The wave forms are similar to each other and the tunnel strain or tunnel deformation due to surface wave is very clear especially in the latter half part. Since the epicenter is located in the direction perpendicular to tunnel axis, these strains were considered to be generated by Love Wave.

Fig. 5 shows the circular strain distribution when body wave is predominant. In this paper, the circular strain is defined as the strain of chord (50 cm in length) fixed on the tunnel wall inside of each cross section. The symbols -45 to +90, i.e., tunnel positions, are illustrated in this figure. It can be noted that when the strain at +45 is positive, the strain at -45 is always negative and furthermore, the strains at +45 and at -45 are larger than those at +00 and +90. Such strain distribution means shear vibration of tunnel cross section due to the first mode shear vibration of the ground at the periphery of tunnel.

Fig. 6 shows the circular strain distribution when surface wave is predominant. The fact that the strains at the top of the tunnel are observed to be the largest means that up-down deformation of tunnel cross-section is being occured. This strain mode repeats cyclically with the period of 4 sec. Therefore, this type of tunnel deformation is most likely caused by surface wave.

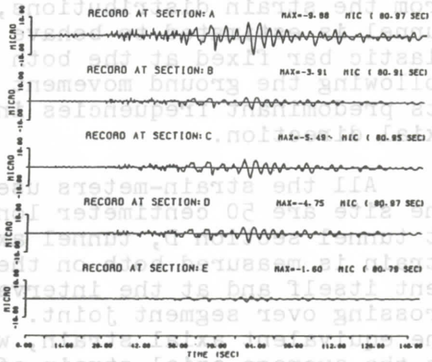

Fig. 4 Axial Strain of Tunnel Wall due to No. 3 Earthquake

CHIBA-IBARAGI KENKYO EARTHQUAKE (NO. 4 EARTHQUAKE)

Fig. 7 shows the ground acceleration record in the direction of tunnel axis. The accelerometers are installed at depths of GL. -1.5 m, -5.0 m, -12.6 m, and -29.8 m respectively. As shown in Fig. 7, body wave is predominant and surface wave does not clearly appear even in the latter half part. The amplification of accelerations at the ground surface to the base ground (mud stone) is about 5 in this earthquake.

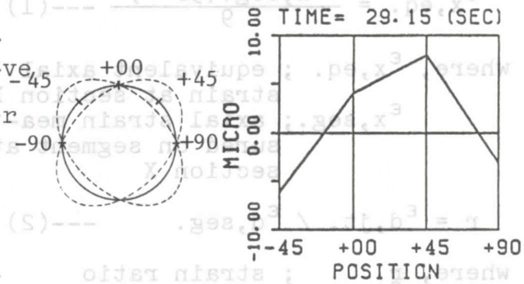

Fig. 5 Circular Strain Distribution (Body Wave)

Fig. 8 shows tunnel axial strai due to No. 4 Earthquake. In contrast with Fig. 4, strain components with long periods can scarcely be seen. It was noted that the wave forms of tunnel axial strains are very similar to those of displacements in the axial direction of the ground at the periphery of a tunnel. As for tunnel circular strains, the strain forms are very similar to those of ground displacements in the direction perpendicular to tunnel axis. And it was recognized that the tunnel circular strain distribution in this case is the same as the shape of Fig. 5 almost all through the observation time.

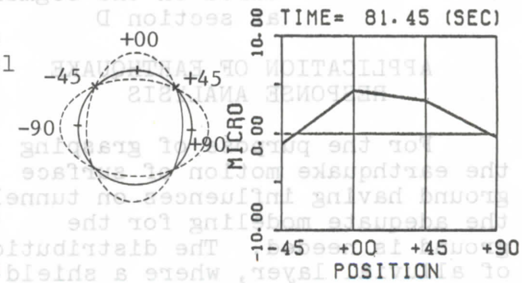

Fig. 6 Circular Strain Distribution (Surface Wave)

Fig. 9 shows tunnel axial strain distribution when a wave peak at tunnel section D exists. Sections A to E in this figure illustrate tunnel sections respectively. A solid line means the axial strain measured at shield segment portion. On the other hand, a dotted line shows the equivalent axial strain calculated, following the manner mentioned in the next paragraph. As shown in Fig. 9 when the strain at D is positive, strain at A is always negative, and vise versa. From the strain distributions, the tunnel is estimated to behave as a elastic bar fixed at the both ends, following the ground movement with its predominant frequencies in the axial direction.

All the strain-meters used at the site are 50 centimeter long. At tunnel section D, tunnel axial strain is measured both on the segment itself and at the interval crossing over segment joint. Thus, the equivalent axial strain, which is the average axial strain of tunnel, is given by the following equation:

$$\varepsilon_{x,eq.} = \frac{\varepsilon_{x,seg.}(5r+4)}{9} \quad \text{---(1)}$$

where, $\varepsilon_{x,eq.}$; equivalent axial strain at section X
$\varepsilon_{x,seg.}$; axial strain measured on segment at section X

$$r = \varepsilon_{d,jt.} / \varepsilon_{d,seg.} \quad \text{---(2)}$$

where, r ; strain ratio
$\varepsilon_{d,jt.}$; axial strain crossing over joint at section D
$\varepsilon_{d,seg.}$; axial strain measured on the segment at section D

APPLICATION OF EARTHQUAKE RESPONSE ANALYSIS

For the purpose of grasping the earthquake motion of surface ground having influences on tunnel, the adequate modeling for the ground is needed. The distribution of alluvial layer, where a shield tunnel is constructed, is very complicated in general cases. Therefore, modeling both an irregular

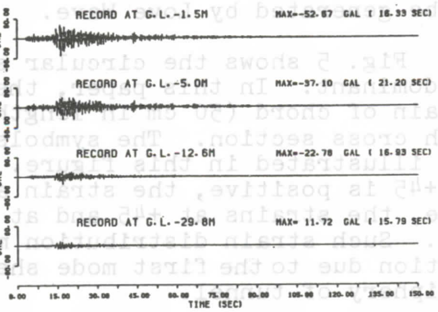

Fig.7 Ground Acceleration Records due to No.4 Earthquake

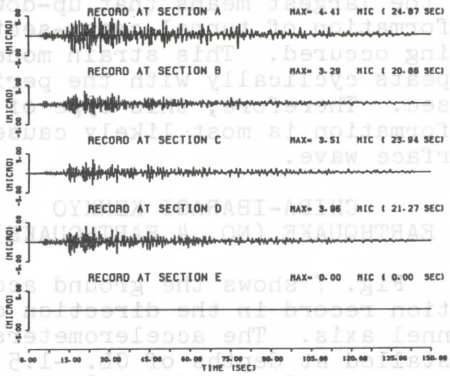

Fig.8 Tunnel Axial Strains Measured at Each Cross Section

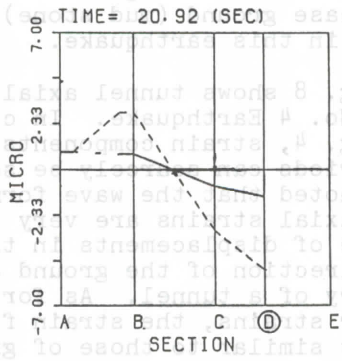

Fig.9 Tunnel Axial Strain Distribution

boundary between alluvium and delvium and soil profiles of alluvial layer is the most important technique, for the response analysis of underground structures. In this chapter, the authors introduce an application of the quasi-three dimensional ground model[3] proposed by the authors, to tunnel axial behavior during No.4 Earthquake at the site mensioned above. The input wave is the ground acceleration recorded at GL.-29.8 m (in mud stone).

Fig.10 shows a mesh, modeling the ground and tunnel at the site. At each intersection of a mesh, a ground mass is laid. Each ground mass is inter-connected by springs and dashpots. The mass is also connected with the base ground by a spring, dealing with the first-mode vibration of a soil pillar. The spring connection system between ground masses can also replaced with FEM. The damping factor used here is 0.05.

Fig.11 shows the maximum equivalent tunnel axial strains obtained by the simulation. In this figure, measured values are also plotted with a symbol *. They show good agreements, thus, it is

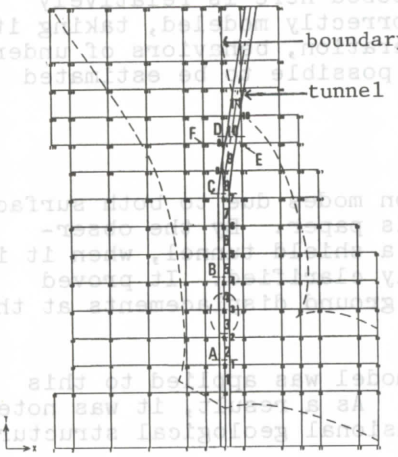

Fig.10 A Mesh Modeling the Observation Site

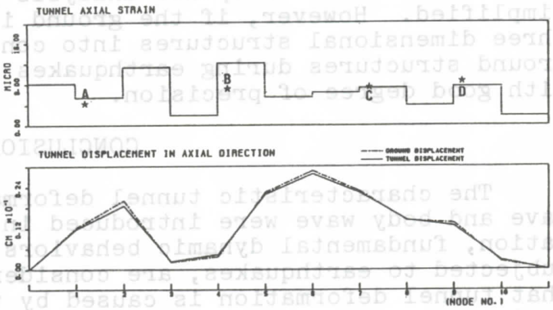

Fig.11 Maximum Equivalent Tunnel Strains and Maximum Displacements of Tunnel and Ground (* -- Measured Strain)

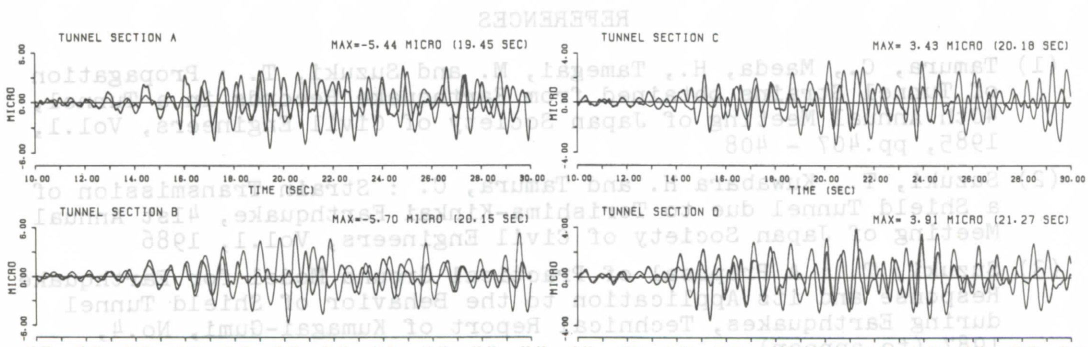

Fig.12 Comparison of Tunnel Strains between Simulation and Observation

noted that the method to model ground and tunnel at the site is adequate. The strain ratio r is about 3.0 in this case. The following equivalent axial rigidity (EA)eq., therefore, was used in the analysis.

$$(EA)eq. = (EA)seg. \frac{9}{5r+4} \qquad (3)$$

where, (EA)eq. ; equivalent axial rigidity of a tunnel
(EA)seg.; axial rigidity of a shield segment ring

Fig.12 shows the comparison between the axial strains of simulation and those of observation. The thick line in this figure shows measured strain and the solid line illustrates simulated strain. It can be said that the time dependent response of tunnel axial deformation is simulated with comparatively good accuracy. This is not limited to No.4 Earthquake. In No.2 Earthquake, where r equals to 9.0, for example, the conformity was satisfactorily observed as well.

The method of response analysis proposed here is relatively simplified. However, if the ground is correctly modeled, taking its three dimensional structures into consideration, behaviors of underground structures during earthquakes are possible to be estimated with good degree of precision.

CONCLUSIONS

The characteristic tunnel deformation modes due to both surface wave and body wave were introduced in this paper. By the observation, fundamental dynamic behaviors of a shield tunnel, when it is subjected to earthquakes, are considerably clarified. It proved that tunnel deformation is caused by the ground displacements at the periphery of a tunnel.

The quasi-three dimensional ground model was applied to this observation site for a response analysis. As a result, it was noted that the ground model, taking three dimensional geological structure into consideration, is necessary.

The authors will continue to carry out the observation in order to confirm the earthquake resistability of a shield tunnel during a large earthquake.

REFERENCES

(1) Tamura, C., Maeda, H., Tamegai, M. and Suzuki, T. : Propagation of Tunnel Strains obtained from Earthquake Records in a Tunnel, 40th Annual Meeting of Japan Society of Civil Engineers, Vol.1, 1985, pp.407 - 408

(2) Suzuki, T., Kuwabara H. and Tamura, C. : Strain Transmission of a Shield Tunnel due to Torishima-Kinkai Earthquake, 41st Annual Meeting of Japan Society of Civil Engineers, Vol.1, 1986

(3) Suzuki, T. : A Proposal of Practical Ground Model for Earthquake Response and its Application to the Behavior of Shield Tunnel during Earthquakes, Technical Report of Kumagai-Gumi, No.4, 1987 (to appear)